The eNOS-dependent S-nitrosylation of the NF-κB subunit p65 has neuroprotective consequences in excitotoxicity.

Ariel Caviedes[1#], Barbara Maturana[1#], Katherine Corvalan, Alexander Engler, Felipe Gordillo[3], Manuel Varas-Godoy[4], Karl-Heinz Smalla[5], Luis Federico Batiz[1], Carlos Lafourcade[1], Thilo Kaehne[2], Ursula Wyneken[1]

[1]Laboratorio de Neurociencias, Centro de Investigación e Innovación Biomédica, Facultad de Medicina, Universidad de Los Andes, Santiago, Chile
[2] Institute of Experimental Internal Medicine, Otto-von-Guericke University, Magdeburg, Germany
[3] Centro de Biotecnología de los Recursos Naturales (CENBIO), Laboratorio de Microbiología Aplicada, Universidad Católica del Maule, Talca, Chile
[4] Cancer Cell Biology Lab, Centro de Biología Celular y Biomedicina (CEBICEM), Facultad de Medicina y Ciencia, Universidad San Sebastián, Lota 2465, Santiago 7510157, Chile
[5]Leibniz Institute for Neurobiology, Magdeburg, Germany

[#] Both authors contributed equally to this work

* Corresponding author: Ursula Wyneken, Laboratorio de Neurociencias, Facultad de Medicina, Universidad de los Andes; Mons. Alvaro del Portillo 12.455, Las Condes; Santiago, Chile; phone: +56 2 26181353; e-mail: uwyneken@uandes.cl
RUNNING TITLE: S-nitrosylation protects from excitotoxicity

Abstract.
Cell death by glutamate excitotoxicity, mediated by N-methyl-D-aspartate (NMDA) receptors, negatively impacts brain function affecting hippocampal, i.e. sensitive neurons. The NF-κB transcription factor (composed mainly of p65/p50 subunits) contributes to neuronal death in excitotoxicity, while its inhibition should improve cell survival. Using the biotin switch method, subcellular fractionation, immunofluorescence and luciferase reporter assays, we found that NMDA stimulated NF-κB activity selectively in hippocampal neurons, while endothelial nitric oxide (eNOS), an enzyme expressed in neurons, is involved in the S-nitrosylation of p65 and consequent NF-κB inhibition in cerebrocortical, i.e. resistant neurons. The S-nitro proteomes of cortical and hippocampal neurons revealed that different biological processes are regulated by S-nitrosylation in susceptible and resistant neurons, bringing to light that protein S-nitrosylation is a ubiquitous post-translational modification, able to influence a variety of biological processes including the homeostatic inhibition of the NF-κB transcriptional activity in cortical neurons exposed to excitotoxicity.

Key words: NMDA, S-nitrosylation, proteomics

Introduction.
Neuronal death by glutamate excitotoxicity is implicated in the pathogenesis of several neurological disorders, ranging from neurodegeneration to epilepsy, stroke and traumatic brain injury (37, 52). The overstimulation of glutamate receptors leads to massive calcium influx, mainly through N-methyl-D-aspartate receptors (NMDA-Rs), triggering several intracellular pro-death signaling pathways (54). Endogenous/homeostatic protective mechanisms in response to glutamate, are incompletely known.
In that line, the nuclear factor kappa B (NF-κB) family of transcription factors has been implicated in excitotoxicity in the retina, the striatum, cerebral cortex and hippocampus (29, 44, 53). This is associated with induction of pro-apoptotic and pro-inflammatory genes, including IL-1β. The canonic activation of the ubiquitous transcription factor NF-κB depends on phosphorylation and degradation of IκB proteins, leading to release and nuclear translocation of NF-κB, a dimer composed most frequently by a p65 and a p50 subunit (10, 22). Its transcriptional activity in the nucleus is regulated by several post-translational modifications, such as phosphorylation and S-nitrosylation (i.e. the reversible coupling of nitric oxide (NO) to cysteine residues). In particular, S-nitrosylation of the p65 cysteine 38 inhibits its transcriptional activity in diverse cell types (24, 41, 46). However, the contribution of this mechanism to excitotoxicity is unknown and might imply a homeostatic regulation of the NF-κB activity. The main source of NO in the brain are nitric oxide synthases, i.e. the neuronal (nNOS), endothelial (eNOS) and inducible (iNOS) enzymes (5, 9, 15). Considering the novel finding that eNOS is present in neuronal cultures and in glutamatergic synapses (6), we examined whether eNOS is involved in p65 S-nitrosylation and thus, in the regulation of its transcriptional activity. For this, we used primary cultures of hippocampal and cortical neurons, which differ in their vulnerability to excitotoxic insults: hippocampal neurons have a higher sensitivity than cortical neurons (45). We found that eNOS contributes to p65 S-nitrosylation and is associated with neuroprotection. This

homeostatic mechanism is not active in hippocampal neurons, in which NF-κB activation after an excitotoxic insult leads to increased nuclear translocation and transcriptional activity, including increased transcription of the pro-inflammatory cytokine IL-1β. Our results show that NF-κB activity can be regulated by an eNOS dependent endogenous neuroprotective mechanism in excitotoxicity.

Materials and Methods.

Material. Chemical reagents were purchased from Sigma (St. Louis, MO, USA), unless otherwise stated. Neurobasal medium (Cat. N◦: 21103-049), B27 (Cat. N◦ 17504-044), MEM (Minimum Essential Medium Cell Culture) (Cat. N° 11900-024), FBS (Fetal Bovine Serum) and Equine Serum (Cat. N° 16050-122) were from Gibco-Invitrogen (San Diego, CA, USA). Penicillin-Streptomycin was from Biological Industries (Cromwell, CT, USA). N-Methyl-D-aspartate (NMDA) (Cat. N° 0114), 6-Cyano-7-nitroquinoxaline-2,3-dione (CNQX) (Cat. N° 0190) and N5-1(1-Iminoethyl)-L-ornithine dihydrochloride (LNIO) (Cat. N° 0546) were from Tocris Bioscience (Bristol, UK). 2-amino-5-phosphonovalerate (APV) (Cat. N° A-169) was from RBI (Natick, MA, USA). Recombinant Escherichia coli-derived BDNF was from Alomone Labs (Jerusalem, Israel). Ro 106-9920 (6-(Phenylsulfinyl) tetrazolo[1,5-b] pyridazine) (Cat. N° 1778), Nimodipine (Cat. N° 482200), S-nitroso-N-acetylpenicillamine (SNAP) (Cat. N° 487910) and 3-amino,4-aminomethyl-2',7'-difluorofluorescein (DAF-FM) (Cat. N° 251515) were from Calbiochem (San Diego, CA, USA). EZ-link HPDP-Biotin (Cat. N° 21341) and Streptavidin Agarose (Cat. N° 20347) were from Thermo Scientific, (Waltham, MA, USA). Trypsin Gold was from Promega (Cat. N° V5280) (Madison, WI, USA).

Antibodies. *Primary antibodies*: Anti-p65 (Cat. N° ab16502), Anti-IκB alpha (Cat. N° ab32518), Anti-Laminin-B1 (Cat. N° 8982), Anti-Tubulin Alpha 1A (Cat N° ab7291) and Anti-GAPDH (Cat. N° ab8245) were from Abcam (Cambridge, UK). Anti-phospho-p65 was from Cell signaling (Cat. N° 3033) (Danvers, MA, USA), Anti-MAP2A/2B was from Millipore (Cat. N° MAB378) (Burlington, MA, USA), Anti-GFAP was from US Biological (Cat. N° G2032-28B-PE) (Swampscott, MA, USA), Anti-βIII tubulin was from Promega (Cat. N° G712A) (Madison, WI, USA), Anti-GluN2A was from Alomone Labs (Cat. N° AGC-002) (Jerusalem, Israel), Anti-SAPAP4 was from Santa Cruz Biotechnology (Cat. N° sc-86851) (Dallas, TX, USA), Anti-Biotin was from Bethyl laboratories (Cat. N° A150-111A) (Montgomery, TX, USA) and Anti-PSD-95 was from BD transduction Laboratories (Cat. N° 610495) (San Jose, CA, USA). *Secondary Antibodies*: HRP Goat anti Rabbit IgG (Cat. N° 926-80011) and HRP Goat anti-Mouse IgG (Cat. N° 926-80010) were from LI-COR Biosciences (Lincoln, NE, USA), Alexa Fluor® 555 goat anti rabbit IgG (Cat. N° A21429) was from Life Technologies (Carlsbad, CA, USA), Alexa Fluor® 488 Goat Anti-Mouse IgG (Cat. N◦ A21202) was from Invitrogen Corporation (Carlsbad, CA, USA).

Neuronal cultures. Primary cultures of cortical (CX) and hippocampal (HP) neurons were obtained from day-18 embryos of Sprague–Dawley rats as described (45), taking into account the ARRIVE guidelines for the use of animals and the rules of the Bioethics Committee of Universidad de los Andes. These cultures were cultivated in the absence of Cytosine arabinoside (AraC) and contained about 30% of astrocytes (31). Excitotoxicity was induced by addition of 30 to 100 μM NMDA and 10 μM glycine for 60 minutes.

Cell fractionation. Cell fractionation was performed immediately after the excitotoxic insult (NMDA + glycine for 1 hour). The whole procedure was performed on ice or at 4°C.

Cells were harvested in buffer A (0.6% NP40 v/v; in mM: 150 NaCl; 10 HEPES pH 7.9; 1 EDTA) and homogenated in Teflon-glass homogenizer, vortexed for 30 seconds and incubated on ice for 10 minutes. This procedure was repeated 3 times. Then, the suspension was centrifuged at 17,000 g by 5 minutes to obtain the cytoplasmatic fraction. The remaining pellet was washed with buffer B (in mM: 150 NaCl; 10 HEPES pH 7.4; 1 EDTA) and centrifuged at 17,000 g by 1 minute at 4°C. The pellet was resuspended in buffer C (25% v/v glycerol; in mM 20 HEPES pH 7.4; 400 NaCl; 1.2 $MgCl_2$; 0.2 EDTA), vortexed for 30 seconds and incubated on ice for 10 minutes (5 times) to finally centrifuge at 17,000 g by 20 minutes to obtain the nuclear fraction.

Cell viability. The percentage of surviving neurons was assessed 24 h after the NMDA challenge using the trypan blue exclusion test, in 24 well plates containing 10,000 cells. Neurons were exposed to 0.05% (v/v) trypan blue in PBS for 5 minutes. The cells were immediately examined under a phase-contrast microscope, and then images of ten random fields near the center of the dish were recorded to quantify the numbers of living neurons (which exclude trypan blue) and dead (stained) neurons.

Immunocytochemistry. Neuronal cultures of 14 to 15 DIV were fixed immediately after the excitotoxic insult with 4% paraformaldehyde in PBS containing 4% of sucrose for 10 minutes and washed with PBS. After fixation the cells were permeabilized with 0.2% Triton X-100 for 5 minutes and washed with PBS containing 25 mM glycine. Cells were incubated with blocking solution (10% BSA in PBS) for 1 h followed by overnight incubation with primary antibody: anti-p65 (1:300), anti-MAP2A/2B (1:1000) and anti-GFAP (1:1000), all diluted in the same blocking solution at 4°C. After incubation with primary antibody, cells were washed with PBS, blocked for 30 minutes with 10% BSA and incubated for one hour at room temperature with the corresponding secondary antibody diluted 1:1000 in blocking solution and finally incubated with DAPI for 5 minutes for nuclear staining. The fluorescence images were obtained using ECLIPSE TE2000U Microscope with NIS-Element imaging software from Nikon Instrument Inc (Minato, Tokio, Japan), and analyzed using Photoshop CS6 software. In order to assess the nuclear translocation of NF-κB by epifluorescence microscopy, 50 cells per condition (control or NMDA) were analyzed in which the nuclear (i.e. DAPI stained) zone was selected and the intensity of p65 was quantified in that area by an experimenter blind to the experimental conditions. Finally, the decodification of the data allowed the comparison of fluorescence intensity of p65 in control and NMDA stimulated cultures.

Knockdown of eNOS. Short hairpin against eNOS (sh-eNOS) was synthesized in integrated DNA technologies (IDT) (Neward, NJ, USA), aligned and expressed in the lentiviral vector pLL3.7-mRuby2, downstream of the U6 promoter and between HpaI and XhoI sites. The sh-eNOS sequence was: 5'-GTGTGAAGGCGACTATCCTGTATGGCTCT-3'. The scrambled RNA (sh-Luc) sequence was: 5'-TTCTCCGAACGTGTCACGT-3'. Correct insertions of the shRNA cassettes were confirmed by restriction mapping and direct DNA sequencing. Lentiviral production was done using lipofectamine 2000 reagent, Promega (Cat. N° 11668-019) (Madison, WI, USA). Briefly, we co-transfected the sh-eNOS or sh-Luc plasmids with the packaging vector Δ8.91 and the envelope vector VSV-g into HEK293T cells in free serum DMEM. 5 hours after transfection the medium was replaced for DMEM containing 10% FBS and the next day the medium was replaced by Neurobasal supplemented with B27. The resulting supernatant containing the lentiviruses was harvested after 48- and 72-hours post-transfection, centrifuged to eliminate cell debris, and filtered through 0.45 mm cellulose acetate filters (Naldini et al., 1996; Dull et al., 1998).

***Nitric oxide production*.** Neuronal cultures were loaded for 1 h at 37ºC with 10 µM 4-amino-5-methylamino-2',7'-difluorofluorescein (DAF-FM) plus 0.015% pluronic acid in recording solution (in mM: 116 NaCl, 5.4 KCl, 0.9 NaH_2PO_4, 1.8 $CaCl_2$, 0.9 $MgCl_2$, 20 HEPES, 10 glucose and 0.1 L-arginine, pH 7.4). Cells were washed 4 times and placed in recording solution. Fluorescence (excitation at 495 nm; emission at 510 nm) were acquired for 500 ms every 5 minutes to minimize the photobleaching of DAF-FM (3). Signals were averaged over regions of interest of somas (excluding the nuclei) and relative intracellular NO levels were calculated from emission at 510 nm. Because there was a linear decay of fluorescence due to photobleaching, the negative slope was determined for each experiment before the addition of the stimulus (BDNF), and the experimental slope was corrected for this (45). At the end of the experiment, the external NO donor S-Nitroso-N-acetyl-DL-penicillamine (SNAP, 10 µM) was applied to check that NO-sensitive dye was still available. Experiments in which SNAP did not increase fluorescence were discarded. Fluorescence was measured using an Eclipse E400 epifluorescence microscope with a FluorX40 water immersion objective (Nikon Corporation, Melville, NY, USA) equipped with a Sutter Lambda 10-2 optical filter changer. Emitted fluorescence was registered with a cooled charge-coupled device video camera (Retiga 2000R Fast 1394, QImaging, Surrey, BC, Canada) and data obtained were processed using imaging software (IPLab 4.0, Scanalytics, Buckinghamshire, UK). For statistical analysis slopes ± SEM of at least four independent experiments were compared by one-way ANOVA followed by a Bonferroni post-test.

Magnetofection of primary neurons. Neuronal cultures of 7 DIV were transfected using magnetic nanoparticles (NeuroMag, Oz Biosciences). Briefly, plasmid DNA of Firefly and Renilla Luciferase were incubated with NeuroMag Transfection Reagent (in a relationship of 2 µl per 1 µg of DNA) in Neurobasal medium and incubated for 20 minutes at room temperature, and then added drop by drop to the culture. Subsequently, the cells were incubated for 15 minutes at 37°C on top of the magnetic plate (Oz Biosciences) and finally, the magnetic plate was removed, and the cells were cultivated in standard conditions.

Dual luciferase assay.

Transfected neuronal cultures with the NF-κB reporter Firefly Luciferase plasmid, which contains a response element to NF-κB, and with a constitutively expressing CMV-Renilla Luciferase plasmid, (Cat. N° E1980, Promega, Madison, WI, USA), were stimulated with 30 or 100 µM NMDA and 10 µM glycine for 60 minutes, in the presence or absence of the NO inhibitor N5-(1-Iminoethyl)-L-ornithine (LNIO). After stimulation, the cells were returned to fresh Neurobasal/B27 medium containing 10 µM CNQX, 2 µM nimodipine and 10 µM APV (to block a-amino-3-hydroxy-5-methylisoxazole-4-propionate (AMPA) receptors, Ca^{2+} channels and NMDA receptors, respectively) during 4 hours to perform the Dual-Luciferase Reporter Assay, according to the manufacturer's protocol and carried out in FLx800 Luminometer, Biotek instrument (Winooski, VT, USA). The data were expressed as the ratio of Firefly to Renilla Luciferase activity (Firefly Luc/Renilla Luc).

Biotin switch method. The protocol of Forrester et al. was applied with minor modifications (Supplementary Figure S1 A-C) (13). Neuronal cultures were homogenized in HENS buffer (in mM: 250 HEPES, 1 EDTA, 0.1 neocuproine, 0.1 % SDS y and protease inhibitors, pH 7.4) plus 100 mM iodoacetamide (IA). Briefly, 1 mg of starting material was blocked with 100 mM of IA in HENS buffer in a final volume of 2 ml in a rotating wheel for 1 h at room temperature, then proteins where precipitated with 3 volumes of acetone at -

20°C (this step was repeated two times). This was followed by overnight pull down of biotinylated proteins with 200 µl of streptavidin-agarose beads in a final volume of 1 ml at 4 °C. Elution was performed with SDS gel electrophoresis loading buffer.

High resolution proteome analysis and label free quantitation. The proteins pulled down in the biotin switch assay were boiled in denaturizing SDS-sample buffer and subjected to SDS-PAGE (n=6 biological replicates for each experimental condition except for hippocampal neurons incubated with NMDA (n=5)). SDS-gels (3% stacking gel, 12% separation gel) were run in a Mini PROTEAN® System (BioRad) at 100 V for 10 min and 200 V till end of the separation. Each lane was divided in eight fractions for in-gel-digestion and further analysis. In-gel digest was performed in an adapted manner according to Shevchenko (47). LC-MS/MS analyses of the generated peptides were performed on a hybrid dual-pressure linear ion trap/orbitrap mass spectrometer (LTQ Orbitrap Velos Pro, Thermo Scientific, San Jose, CA) equipped with an EASY-nLC Ultra HPLC (Thermo Scientific, San Jose, CA). Peptide samples were dissolved in 10 µl 2% ACN/0.1% trifluoric acid (TFA) and fractionated on a 75 µm I.D., 25 cm PepMap C18-column, packed with 2 µm resin (Dionex, Germany). Separation was achieved through applying a gradient from 2% ACN to 35% ACN in 0.1% FA over a 150 min gradient at a flow rate of 300 nl/min. The LTQ Orbitrap Velos Pro MS has exclusively used CID-fragmentation when acquiring MS/MS spectra consisted of an Orbitrap full MS scan followed by up to 15 LTQ MS/MS experiments (TOP15) on the most abundant ions detected in the full MS scan. Essential MS settings were as follows: full MS (FTMS; resolution 60.000; m/z range 400-2000); MS/MS (Linear Trap; minimum signal threshold 500; isolation width 2 Da; dynamic exclusion time setting 30 s; singly-charged ions were excluded from selection). Normalized collision energy was set to 35%, and activation time to 10 ms. Raw data processing and protein identification of the high resolution Orbitrap data sets was performed by PEAKS software suite (Bioinformatics Solutions, Inc., Canada). False discovery rate (FDR) was set to < 1%.

Western blotting. Twenty micrograms of protein of each sample, dissolved at 1 mg/ml in loading buffer, were separated by sodium dodecyl sulfate–polyacrylamide electrophoresis (SDS–PAGE) on 10% gels under fully reducing conditions and transferred onto nitrocellulose membranes. Membranes were incubated overnight at 4°C with primary antibodies followed by incubation at room temperature with secondary antibody conjugated with horseradish peroxidase for 60 min. Immunoreactivity was visualized using the ECL detection system. Densitometric quantification was performed using the image processing program ImageJ (National Institute of Health, USA). Data were expressed as fold change from homogenate for at least 4 independent preparations and mean ± SEM for each fraction was calculated.

Quantitative PCR. Total RNA from primary hippocampal cultures was extracted using TRizol reagent from Life technologies (Carlsbad, CA, USA), 1 µg of RNA was reverse transcribed into cDNA using MultiScribe reverse transcriptase from ThermoFisher (Waltham, MA, USA) according to the manufacturer's protocol. Quantitative polymerase chain reaction (qPCR) reaction was carried out using the Brilliant III Ultra-Fast QPCR Master Mix in the Stratagene Mx3000P system (Agilent Technologies, Santa Clara, CA, USA). The thermal cycling protocol was: pre-incubation, 95°C, 10 min; amplification, 40 cycles of (95°C, 20 s; 60°C, 20 s; 72°C, 20 s); melting curve, 1 cycle of (95°C, 1 min; 55°C, 30 s; 95°C, 30 s). qPCR was performed using triplicates. Primers used were: rat IL-1β, forward primer 5′ TCAGGAAGGCAGTGTCACTCATTG 3′ and reverse primer 5′ ACACACTAGCAGGTCGTCATCATC 3′. The results were normalized against rat mRNA

of GAPDH, Forward primer 5′ TTCACCACCATGGAGAAGGC 3′ and reverse primer 5′ GGCATGGACTGTGGTCATGA 3′. The gene expression was represented by the value of ΔCt (Sample Problem Ct – Reference Gene Ct). The relative expression is expressed as fold change over control using the $2^{-\Delta\Delta Ct}$ expressed on base 2 logarithmic scale.

Statistical Analysis. Average values are expressed as means ± SEM. Statistical significance of results was assessed using two-tailed Student's t-test or one-way ANOVA followed by Bonferroni post-tests, as indicated. All statistic data of the experiments shown here are summarized in Supplementary Table 1.

Results.

NF-κB activation in cortical and hippocampal cell cultures after NMDA stimulation.

To assess the participation of NF-κB in excitotoxicity, we studied the activation and nuclear translocation of p65 in NMDA-stimulated cortical and hippocampal cell cultures (Figure 1). These cell cultures are mixed and they contain approximately 30% of astrocytes (31). We first assessed cell viability following incubation with different NMDA concentrations (Supplementary Figure S1 D): in our experimental conditions, 30 μM NMDA did not induce significant cell death thus representing a mild excitotoxic stimulus, in which excitotoxicity-associated pathways are initiated without provoking cell death within 24 hours. In contrast, 100 μM NMDA was able to produce significant cell death, representing a strong excitotoxic stimulus that leads to cell death within 24 hours. In control and NMDA-stimulated cultures, we first quantified the nuclear translocation of p65. Based on the distribution of a nuclear (i.e. Laminin B, enriched in the nuclear fraction by 18.6 ± 2.8 times over homogenate) and a cytoplasmic (i.e. GAPDH) marker among fractions we could conclude that a reliable separation of nuclei from cytoplasm was obtained (Supplementary Figure S1 E). In Figure 1A and B, representative Western blots of p65 and its phosphorylated form in the nuclear fractions are shown, while Laminin B was used as a loading control. Note that p65 phospho-serine 536 is considered as general marker of NF-κB activation, especially of the canonic pathway (20). The densitometric analysis of the Western blots (Figure 1 C and D) confirmed that p65 increased in the nuclear fractions of hippocampal neurons (HP, white bars) but not in cortical neurons (CX, black bars) exposed to the same excitotoxic conditions/NMDA concentrations. Interestingly, this was not accompanied by any changes in the levels of phospho-serine 536, indicating that the nuclear translocation of p65 in our experimental model was independent of this phosphorylation site. To determine whether astrocytes contributed to nuclear translocation in the hippocampal cultures, we used immunofluorescence to detect p65 in DAPI-stained nuclei in neurons (labelled with an antibody against microtubule associated protein 2, MAP2) or astrocytes (labelled with an antibody against glial fibrillary associated protein, GFAP) (Supplementary Figure S2). Consistent with the previous observations, we found that NMDA induced an increase in the nuclear content of p65 in both neurons and astrocytes. No translocation was observed in cortical cell cultures in both cell types.

To evaluate the transcriptional activity of NF-κB, we used the NF-κB luciferase reporter assay (Figure 1 E and F). Consistent with the previous results, NF-κB transcriptional activity increased in hippocampal neurons exposed to 100 μM NMDA while no effects were observed in cortical cells. To test whether NF-κB activation is associated with cell death, we used the NF-κB inhibitor Ro 106-9920 (Figure 2) at a concentration of 2 μM, not affecting neuronal cell survival per se (Figure 2A). As expected (Figure 2 B and C), 100

μM NMDA induced cell death in hippocampal neurons. This was prevented by NF-κB inhibition with Ro106-9920. Surprisingly, cell death in the cortical cultures (i.e. resistant to 100 μM NMDA) increased in the presence of the NF-κB inhibitor, suggesting opposing roles in neurotoxicity/neuroprotection of NF-κB in both cell types.

S-nitrosylation of p65 increased in cortical cell cultures after NMDA.

We hypothesized a regulation of the NF-κB p65 subunit in the used excitotoxicity model by S-nitrosylation. To prove this, we used the biotin switch assay (13) to identify proteins containing nitrosylated cysteine residues. Efficacy of all protocol steps were controlled by Western blot and protein staining (Supplementary Figure S1 A-C). Interestingly, the pull down revealed that S-nitrosylation of p65 increased after NMDA in cortical cells, while in hippocampal cells the opposite effect was observed (Figure 3). This result supports the idea that S-nitrosylation is a dynamic post-translational modification regulating p65 activity. In addition, considering the literature, an increased p65 S-nitrosylation is associated with decreased transcriptional activity in other cell types and experimental models. To further evaluate the observed p65 S-nitrosylation and their putative functional effects in our model, we directly altered p65 S-nitrosylation by decreasing NO levels by inhibition of nitric oxide synthases (NOS). First, we focused particularly on eNOS, previously described by us to be expressed in neurons (6). We measured the eNOS-dependent NO production using the NO sensitive fluorescence probe DAF-FM in cortical cultures transfected with a shRNA targeting eNOS (Figure 4 A and B) (6). To stimulate NO production, the neurotrophin BDNF was used (45). In the presence of the sh-eNOS RNA (but not of a sequence targeting Luciferase as a control), the production of NO decreased significantly, as revealed by the respective slopes. Following, we tested whether decreased endogenous NO production could affect the S-nitrosylation of p65 and tubulin 1A, that have been shown in several studies to be NO targets (14, 38) (Figure 4 C and D). In fact, after using the biotin-switch assay of neuronal cultures transfected with sh-eNOS RNA it was shown that the S-nitrosylation of p65 decreased markedly with respect to the sh-Luc as controls in cortical or hippocampal cultures, respectively. In turn, tubulin 1A S-nitrosylation also decreased significantly with respect to sh-Luc. Thus, we conclude that eNOS significantly contributes to the observed protein S-nitrosylation and that inhibition of its activity leads to decreased S-nitrosylation of selected proteins.

NO regulates transcriptional activity of NF-κB but not its nuclear translocation in response to NMDA stimulation.

Although it is known that NO inhibits the transcriptional activity of NF-κB (46), this type of regulation has not yet been observed in neurons. Moreover, it is unknown whether NO affects nuclear translocation. Therefore, we measured nuclear translocation and NF-κB activity using the NOS inhibitor LNIO (Figure 5). In Figure 5 A, it is shown in nuclear fractionation experiments followed by Western blots that the levels of p65 did not change among the experimental conditions in cortical cells. Moreover, in hippocampal cells nuclear p65 increased after 100 μM NMDA, which could not be prevented by LNIO application. This suggests that nuclear translocation of p65 was not affected by S-nitrosylation. To evaluate putative changes in p65 expression levels, we compared total p65 within the cellular homogenates. The invariable expression levels clearly indicate that the increased nuclear content is a result of enhanced translocation (Supplementary Figure S3 A and B). In that line, we also measured the IκB-α levels in the cytoplasm, but we did not find significant differences among groups (Supplementary Figure S3 C and D).

To further investigate whether NOS inhibition affected the transcriptional activity of NF-κB, we used the luciferase reporter system (Figures 5 C and D). In cortical cells, the presence of LNIO led to increased transcriptional activity in NMDA-stimulated cells. Similar effects were observed in hippocampal cells. This suggests that NOS-dependent NO synthesis leads
to NF-κB inhibition. To further prove that NF-κB could be inhibited by NO in hippocampal cells, we measured NF-κB activity in the presence of the NO donor SNAP (Figure 5 E). As expected, SNAP had an inhibitory effect on NF-κB.
We finally investigated whether NF-κB activation in hippocampal neurons was associated with enhanced transcription of known NF-κB regulated genes, measuring mRNA levels of its downstream pro- or anti-apoptotic genes (BAX, Caspase 11, Bcl2) using qPCR. Surprisingly, we did not detect any changes in the mRNA levels of these genes (not shown), while changes were observed in the mRNA levels of the pro-inflammatory cytokine IL-1β: in time course experiments, we could detect that IL-1β increased after 2 hours of stimulation with 100 μM NMDA (Supplementary Figure S4), and this was inhibited in the presence of the NF-κB inhibitor Ro 106-9920 (Figure 5 F). Interestingly, in a different set of experiments it was observed that the NO donor SNAP also inhibited the increased transcription of IL-1β after NMDA (Figure 5 G). These results suggest that the NF-κB activation in hippocampal neurons induces the transcription of the pro-inflammatory cytokine IL-1β while this can be prevented using an NO donor to promote the inhibitory S-nitrosylation of NF-κB. Alternatively, other regulatory proteins of the NF-κB pathway could be NO targets as well. In order to assess whether S-nitrosylation can be considered a more general mechanism regulating the outcome of excitotoxic stimuli, we detected the S-nitrosylation proteome in cortical and hippocampal cultures after NMDA stimulation.

Detection of S-nitrosylated proteins by mass spectrometry.

Hippocampal and cortical cultures were incubated in the presence or absence of NMDA to pull down S-nitrosylated proteins using the biotin switch assay (Figure 6). Interestingly, we found that in hippocampal neurons, a lower number of proteins were detected (in total, 178 proteins were found in hippocampal neurons while in cortical neurons, 360 proteins were identified) (Figure 6A and Supplementary Table 2). To exclude technical issues resulting in lower number of proteins in hippocampal cultures, we carefully controlled that equal quantities of inputs were used (i.e. Supplementary Figure S1). These results suggest that protein S-nitrosylation levels are elevated in cortical neurons both under control and excitotoxicity conditions compared to hippocampal cultures. The respective Venn diagrams (Figure 6 C) revealed in addition that in cortical cultures, 41 and 64 proteins were identified exclusively in control or NMDA-stimulated cortical cultures, respectively, while in hippocampal neurons (Figure 6 D), 8 and 40 exclusive proteins were found. Interestingly, after NMDA 226 proteins were exclusive to cortical and 77 proteins to hippocampal cultures (Figure 6 B), suggesting that the biological processes regulated by protein S-nitrosylation after NMDA are quite different in both cell types. To find out which biological processes were selectively affected by NMDA in both culture types, a meta-analysis using the list of proteins obtained after NMDA stimulation revealed that different biological processes were affected in each case (Figure 6 E). Interestingly, in cortical cells, the S-nitrosylation (and consequent inhibition) of the proteasome subunits may contribute to decreased proteasomal degradation of the the NF-κB inhibitor IκBα, thus providing an additional level of NF-κB inhibition in cortical excitotoxicity (23, 28). On the other hand,

in hippocampal neurons a functional cluster involved in actin filament capping or brain development stand out. In neurons, the actin cytoskeleton plays a major role in several functions including membrane remodeling and organelle trafficking in a motor-dependent (i.e. myosin) or independent form (27). The role of S-nitrosylation of the actin cytoskeleton associated regulatory or motor proteins has not yet been assessed in neurons, although in cardiomyocytes, S-nitrosylation of several of them lead to inhibition, i.e. lower calcium sensitivity and decreased muscle contraction (12, 21, 36).

We also determined whether a differential protein S-nitrosylation in both culture types could be detected in already well-validated NO targets. Thus, we quantified the S-nitrosylation of the NMDA receptor subunit GluN2A (8) and the scaffolding protein PSD95 (19). Furthermore, we included the synapse associated protein SAPAP4, a scaffolding protein that had been detected by us in a previous S-nitrosyl proteome (not published) (Figure 6 F and G). The S-nitrosylation of the synaptic proteins GluN2A and PSD95 were increased in both culture types. Interestingly, S-nitrosylated SAPAP4 increased in cortical cultures while no changes were observed in hippocampal cells, showing that in addition to p65, NO has different protein targets in both cell types.

Finally, our results can be summarized in the model presented in Figure 7.

Discussion.

In this work, we show a neuroprotective pathway involving eNOS-dependent p65 S-nitrosylation. In that line and in concordance with our results, NO has been proposed as a promising therapeutic strategy after excitotoxic insults in the developing brain (39). Moreover, in several preclinical models of ischemic stroke followed by reperfusion or of traumatic brain injury, increasing eNOS-dependent NO production or the cerebral NO levels either using NO donors or NO inhalation has neuroprotective effects (16). These positive outcomes may be in part due to improved blood flow, but also to cellular responses. Thus, our paper contributes importantly to the understanding of a neuronal mechanisms that participates in NO mediated neuroprotection in acquired brain injuries. This may help to propose novel therapeutic strategies aiming at inhibiting harmful NF-κB activity, e.g. during aging (57).

Possible pathways that regulate eNOS-dependent NO production in cortical cells and in the cerebral cortex.

eNOS in the endothelium can be activated in complex ways, from shear stress to a variety of calcium-mobilizing agonists that bind to cell surface receptors, including transmembrane tyrosine kinase receptors (11). In that line, the neurotrophin BDNF and its receptor TrkB, a signaling system associated importantly with improvement of cognitive functions in the central nervous system, is known to activate eNOS in endothelial cells (32, 33). Thus, we used BDNF to stimulate eNOS-dependent neuroprotective NO synthesis in our cell model. Consistent with our results, the restitution of BDNF/TrkB signaling after a stroke enhanced neuroprotection in the cerebral cortex (51). Moreover, further current studies have implicated neuronal expression of eNOS and its role in neuronal adaptations (49). We focused on NF-κB, a known target of NO and also implicated in opposing neuroprotective or neurotoxic effects. Specifically, NF-κB activation favored cell death or damage in pathophysiological models that involve NMDA excitotoxicity (25, 42, 56). Consistent with this idea, NF-κB inhibition by S-nitrosylation resulted in neuroprotection in our excitotoxicity model.

Constitutive NF-κB activity has been described in different brain areas, such as in the cerebral cortex, hippocampus, amygdala, cerebellum, hypothalamus and olfactory bulbs

(10, 22). In *in vivo* experiments, using a transgenic mouse model in which NF-κB expression was measured by β-galactosidase activity, high constitutive expression was found in the CA1, CA2 and dentate gyrus regions of the hippocampus, while lower levels were found in the cerebral cortex (4). This constitutive activity is beneficial for neuronal survival as well as for learning and memory and thus, might favor the transcription of genes involved in these processes. It is unknown why an excitotoxic insult switches NF-κB activity to the expression of deleterious or pro-inflammatory proteins (26). One possibility is that different post-translational modifications that act in concert, also known as the "bar code" for NF-κB activation, determines this switch (40). In addition to p65, it has been reported that the p50 subunit of NF-κB can be S-nitrosylated at the highly conserved cysteine 62, and similarly to p65 modification, this results in the inhibition of its DNA binding capacity. In consequence, S-nitrosylation of the p50 subunit also contributes to NF-κB inhibition (30, 41, 46). Another component of the NF-κB pathway which can be S-nitrosylated is the inhibitor of NF-κB (IκB) kinase (IKK) complex, the main kinase complex responsible for the phosphorylation of the IκB-α protein. The IKK complex is composed by the two catalytic subunits IKK-α and IKK-β and the regulatory subunit IKK-γ. The S-nitrosylation of the cysteine 179 of the IKK-β subunit results in the inhibition of the kinase activity of the IKK complex and consequently the lack of IκB-α protein phosphorylation, thus preventing activation of NF-κB (43). In such a way, enhanced protein S-nitrosylation of the different NF-κB pathway components converge on its inhibition. Due to the very low abundance of NF-κB molecules and their regulators compared to other proteins, e.g. those of the cyoskeleton, we failed to detect them in the performed mass spectrometric screens of S-nitrosylated proteins. Remarkably, even the up to date most sensitive approach for S-nitrosylation (Cys-BOOST), i.e. bioorthogonal cleavable-linker based enrichment and switch technique wasn't capable of detecting any NF-κB related molecules so far (34). Moreover, when separating neuronal cell nuclei to obtain enrichment of S-nitrosylated nuclear proteins and a higher chance to detect less abundant proteins, NF-κB remains hidden (48).

The SNO proteome after excitotoxicity.

S-nitrosylation of proteins is the principal cGMP-independent mode of action of NO. The S-nitrosylation of redox-sensitive cysteins has been described in thousands of proteins that regulate a variety of biological functions (34, 50). In total the here performed MS-based S-nitrosylation screens identified 445 different proteins. Hierarchical GO-based clustering of those proteins (Supplementary Table 3) revealed the strongest belongings to metabolic processes, including glycolysis, tricarboxylic acid cycle, 2-oxoglutarate process, ATP biosynthetic process and carbohydrate metabolic process. This ranking was followed by increased S-nitrosylation of mitochondrial proteins modulating their function including negative effects on electron transport chain, alteration in mitochondrial permeability transition and enhanced mitochondrial fragmentation and autophagy (18). However, synapse associated processes, like synaptic transmission, neurotransmitter transport, ionotrophic glutamate receptor signaling, neuron projection development and brain development are within the top 35 of this list. This indicates that beside metabolic processes even basic neuronal mechanisms are regulated by S-nitrosylation. The current view is that under conditions of normal NO production, S-nitrosylation regulates the activity of many normal proteins but increased levels of NO, as experimentally induced by

lasting NMDA stimulation, led to aberrant S-nitrosylation, thus contributing to the pathogenesis of neurodegenerative and other neurological disorders (35). Remarkably, in this context we found increases in the GO terms “protein phosphorylation” and “protein autophosphorylation” (Supplementary Table 3) after NMDA stimulation. The found SNO modified proteins belonging to these terms include important serine kinases, including CAMK2d, GSK3ß, AKT1 and MAPKinases but also tyrosine kinases like FYN and SRC. It is already well established, that SNO modification of SRC overrides an inhibitory phosphorylation motif and lead to a phosphorylation independent activation of this kinase, resulting in the activation of various signaling cascades (1, 2). Moreover, CAMKII, one of the most important neuronal kinases that is activated in dendritic spines by calcium influx through the NMDA receptor and heavily implicated in long-term potentiation (LTP), was also found as a S-nitrosylated protein after NMDA stimulation. Surprisingly, S-nitrosylation of CAMKII can induce a Ca^{2+}independent activation (7). This could lead to a sustained activity of signaling cascades by locking the CAM-kinase into an activated state. However, other studies describe the opposite effect namely an inhibition of CAMKII autophosphorylation after S-nitrosylation (55). It is beyond doubts that S-nitrosylation can strongly modulate the activity of key kinases in neurons that in turn, are known NF-κB regulators (10, 17).

Our study has shown that excitotoxicity in general results in a substantially modified SNO proteome of neurons. In them, protein clusters that regulate the NF-κB pathway were found: e.g. S-nitrosylation of proteasomal proteins causes its inhibition and in consequence, a decreased degradation of IκB should be expected thus contributing to NF-κB inhibition (23, 28). The work presented here encourage therapeutic strategies to inhibit NF-κB to favor homeostatic adaptations to excitotoxicity, an idea that is supported by the positive outcomes of NF-κB inhibition in aging to increase health- and lifespan (57).

Acknowledgements: We thank Albert M Galaburda for critically reading the manuscript.

Data Availability: The data that supports the findings of this study are available in the supplementary material of this article

Author Contribution: UW and TK designed the experiments and wrote the manuscript, AC prepared the final version of all figures and of the manuscript. FB, CL and KHS revised carefully the manuscript. MV designed molecular tools and supervised experiments (eNOS knockdown and dual luciferase assay). FG initiated biotin switch assay. The experimental work was done by: Figure 1, KC generated data of panels A-D, AC generated E-F; Figure 2, generated by KC; Figure 3, generated by BM; Figure 4, generated by AC; Figure 5, generated by AC and KC; Figure 6, BM did the biotin switch and generated the data of A to D, F, G; TK supervised the mass spectrometry; AE did the bio-informatic analysis.

Competing Financial Interests
All authors declare that they have no conflict of interests

FIGURE LEGENDS

Figure 1.- NF-κB is activated in hippocampal, but not in cortical cultures after incubation with NMDA. **A)** and **B)** Neuronal cultures were stimulated with 30 µM or 100 µM NMDA for 1 hour and nuclear fractions were separated subsequently. Representative Western blots of cortical (A) and hippocampal (B) culture-derived nuclear fractions after stimulation with 30 µM (top) or 100 µM (bottom). For each Western blot, equal quantities of proteins were loaded and Lamin B1 (LamB) was used as loading control. **C)** and **D)** Densitometric quantification of relative changes of p65 (C) and phospho-p65 (D) in the nuclear content, comparing stimulated (NMDA) vs control (non-stimulated) condition in the same Western blot. Calculated results obtained of 6 independent experiments (n=6). Statistical significance was assessed by two-tailed t-test (* $p<0.05$; ** $p<0.01$). **E)** and **F)** Showing relative luciferase activity in cortical (E) and hippocampal (F) neurons after stimulation with 30 µM or 100 µM NMDA for one hour (n=6). Statistical significance was assessed by One-way ANOVA followed by Bonferroni post-test (**$p<0.01$).

Figure 2.- Inhibition of NF-κB with Ro 106-9920 decreases cell viability in cortical cultures but increases it in hippocampal cell cultures. A) Effect of different concentrations of 6-(Phenylsulfinyl)tetrazolo[1,5-b]pyridazine (Ro 106-9920) on cell viability of cortical and hippocampal cultures **B) and C)** A concentration of 2 µM Ro-106-9920, chosen because it does not affect cell viability per se, was used in 30 µM (B) or 100 µM (C) NMDA stimulated cultures for one hour. Cell death was detected by Trypan blue exclusion test. Results obtained in n=4 independent experiments. Statistical significance was assessed by One-way ANOVA followed by Bonferroni post-test * $p<0.05$; ** $p<0.01$; *** $p<0.001$.

Figure 3.- Different levels of NF-κB p65 subunit S-nitrosylation (-SNO) in cortical (CX) and hippocampal (HP) cell cultures after stimulation with NMDA. Neuronal cultures were stimulated with 30 µM NMDA for one hour. Afterwards, cells were homogenized to pull down S-nitrosylated proteins using the biotin switch assay. Representative Western blots of the S-nitosylated p65 subunit of NF-κB and densitometric quantification of cortical and hippocampal cell cultures are shown comparing stimulated (NMDA) vs control (non-stimulated) condition in the same Western blot. n=4 independent experiments and statistical significance was assessed by two-tailed t-test. ** $p<0.01$; *** $p<0.001$, # $p<0.01$.

Figure 4.- eNOS contributes to NO production and S-nitrosylation of selected proteins. A) Relative increase of NO after the addition of 200 ng/ml BDNF to cortical cell cultures previously transfected with a shRNA targeting eNOS, sh-Luc shRNA or not

transfected controls. **B)** Mean slopes of NO production are shown in n= 4 to 6 independent experiments, * p<0.5 by two-way ANOVA followed by Bonferroni post-test. **C)** The biotin-switch assay was used to pull down S-nitrosylated proteins. Western blots detecting p65 subunit and tubulin 1α in the pull downs of cortical and hippocampal cultures are shown. Cell cultures were transfected with shRNA targeting eNOS or scrambled shRNA. **D)** Densitometric quantification of the S-nitrosylated (SNO) levels of NF- κ B subunit p65 and tubulin α-1A. Result obtained from n= 4 to 6 independent experiments. * p<0.05; ** p<0.01; *** p<0.001 by two-tailed t-test. CX: cortical cultures; HP: hippocampal cultures; Control: not transfected cortical neurons. Sc= scrambled shRNA sequence, eNOS = short interfering RNA against eNOS, C – is a negative control for the biotin switch assay (pull down of samples in which reduction with ascorbate was omitted).

Figure 5.- Nitric monoxide decreases transcriptional activity and gene expression but not nuclear translocation of NF-κB in response to NMDA stimulation. A) and B) Representative Western blots and densitometric quantifications of nuclear content of p65 in cortical (A) and hippocampal (B) cultures stimulates with NMDA (100 µM) in presence or absence of NO inhibitor LNIO (N5-(1-Iminoethyl)-L-ornithine). For each Western blot, equal quantities of protein were loaded and Lamin B1 (LamB) was used as loading control for nuclear fraction. All results were obtained in n=5 independent experiments. * p<0.5; ** p<0.1 by two-way ANOVA followed by Bonferroni post-test. **C) and D)** Relative luciferase activity in cortical (C) and hippocampal (D) neurons after NMDA 30 µM and 100 µM stimulation in presence and absence of LNIO. E) Relative luciferase activity in hippocampal neurons after NMDA 100 µM stimulation in presence and absence of NO donor SNAP (S-nitroso-N-acetylpenicillamine). All results were obtained in n=6 to 10 independent experiments. Statistical significance was assessed by One-way ANOVA followed by Bonferroni post-test. * p<0.5; ** p<0.1; *** p<0.001. F and G) IL-1B mRNA measured by quantitative PCR in hippocampal cultures 2 hours after NMDA 100 µM stimulation in presence or absence of Ro 106-9920 or SNAP. Bar graph showing the mean ± SEM fold change normalized against GAPDH as reference. Data obtained from 4 to 8 independent hippocampal cell culture experiments. Statistical significance was assessed by One-way ANOVA followed by Bonferroni post-test. **p<0.01; ***p<0.001.

Figure 6.- Identification of S-nitrosylated proteins after NMDA stimulation by nanoLC-MS/MS.
S-nitrosylated proteins in hippocampal and cortical cultures were identified by mass spectrometry (n=6 except hippocampal neurons incubated with NMDA (n=5)). A remarkable larger number of S-nitrosylated proteins were detected in cortical neurons than in hippocampal. **A)** Venn Diagrams showing the distribution of proteins in cortical vs. hippocampal cultures (using the sum of identified proteins in both, control and NMDA stimulated cultures). **B)** cortical vs. hippocampal cultures, using proteins identified under NMDA stimulation. **C)** Proteins identified in control vs NMDA stimulated cortical cultures **D)** Proteins identified in control vs NMDA stimulated hippocampal cultures. In C and D,

only proteins were considered which were detected at least two times under each experimental condition. CX= cortical cell cultures, HP=hippocampal cell cultures. **E)** Meta-analysis of proteomic data using GeneCodis. Identified proteins exclusively detected in cortical (red) or hippocampal (green) proteomes were functionally annotated using the web-based tools GeneCodis and Gene Ontology (GO). A single enrichment analysis of biological processes was performed with each list of proteins. The obtained data were visualized by building a graph where the nodes are the proteins that are annotated with the enriched biological processes terms from Gene Ontology. The connections where made by looking at the enriched terms the Proteins where annotated with. If two proteins had the same annotation in common, a line was drawn. When two different colored nodes i.e. proteins are not connected they don't share the same biological processes. To emphasize the similarities a force field embedder was used to layout the graph, depicting similar proteins closer to each other. Note that S-nitrosylation controls different cellular pathways. **F)** Validation by Western blot of S-nitrosylated proteins that were pulled down with the biotin switch method. **G)** Densitometric quantification of S-nitrosylated (-SNO) proteins in cortical (CX) and hippocampal (HP) cultures after NMDA stimulation, in n=4 independent experiments. # $p<0.05$; * $p<0.05$; ** $p<0.01$; *** $p<0.001$.

Figure 7.- Proposed model summarizing the results. Induced/activated eNOS located at the excitatory synapse produces NO, leading beside others to NF-κB S-nitrosylation in cortical cells and inhibiting NF-κB-dependent gene expression. However, under excitotoxic conditions this eNOS-dependent negative regulation of p65 is not present in hippocampal cultures. Therefore, NMDA leads to the activation and nuclear translocation of NF-κB, resulting in a transcriptional activation that includes pro-inflammatory genes, including IL-1β. The transcriptional activity of NF-κB can be selectively induced in cortical cultures by inhibiting NOS enzymes with LNIO. Likewise, in hippocampal cultures, the transcriptional activity (including IL-1β transcription) can be inhibited by the NO donor SNAP.

SUPPLEMENTARY TABLE LEGENDS

Supplementary Table 1. Statistics of all experimental data.

Supplementary Table 2. Protein list of all identified proteins. The columns indicate the protein name, the entry name and the number of detections of the protein in hippocampal and cortical neurons in control or NMDA-stimulated cultures.

Supplementary Table 3. Filtered Genecodis results: Single enrichment analyses were performed with Genecodis on the SNO-proteome data of the NMDA stimulated and unstimulated rats. The resulting lists were merged via their Gene Ontology Terms (biological processes). A cut-off for the adjusted p-values was set at 0.01 and p-values cells were filled grey, if and only if the p-values were at least $1x10^{-1}$ apart, marking the group with potentially more proteins dedicated to the biological process.

SUPPLEMENTARY FIGURE LEGENDS

Supplementary Figure S1. Methodological aspects: A to C: Biotin switch assay in neuronal cell cultures, D: NMDA doses and cell death in cell cultures, E: obtention of nuclear fractions. A) Biotin switch assay. Free –SH groups were blocked in 1 mg of starting material 2 times with 100 mM iodoacetamide for one hour at room temperature, followed by reduction of S-nitrosylated cysteines with 100 mM sodium ascorbate and subsequent labeling them with 300 µM biotin HPDP for one hour. Biotinylated proteins were considered as formerly S-nitrosylated ones and pulled down by streptavidin-beads. The figure was based on Forrester et al. (13). In the negative control (C-), sodium ascorbate was omitted and thus, finally no biotinylated proteins are expected. B) Detection of the biotinylated proteins by Western blot using an anti-biotin antibody in cortical and hippocampal cultures, showing correct -SH group blocking and biotin labeling. C) Silver staining of biotinylated proteins captured by streptavidin beads and separated in a 10 % SDS–PAGE. **D) Dose response curve for NMDA.** Cell viability was assessed at different NMDA concentrations, applied for one hour to measure cell death with the Trypan exclusion test 24 hours later. Hippocampal (HP) or cortical (CX) cultures were studied. 30 µM NMDA stimulation induces no significant cell death, analyzed in n= 3 to 4 independent experiment. Statistical significance was assessed by One-way ANOVA followed by Bonferroni post-test. **$p<0.01$; *$p<0.05$. **E) Nuclear fractionation.** Approval of sufficient purification of prepared nuclear fractions by the nuclear marker Laminin B1. Representative Western blot of total levels of Lamin B1 and GAPDH (as cytoplasmic marker) in subcellular fractions: homogenate, and the cytoplasmic and nuclear fractions. An enrichment of Lamin B1 and absence of GAPDH in the nuclear fraction is observed. The densitometric quantification (fold change in the nuclear fraction over homogenate) of Lamin B1 is shown (n=13 biological replicates). **** $p<0.0001$ by two-tailed t-test. Homo=homogenate; Cyt= cytoplasmic fraction; Nuc= nuclear fraction.

Supplementary Figure S2. NMDA induces the nuclear translocation of p65 (NF-κB) in hippocampal but not in cortical cultures. Neurons (top panel) and Astrocytes (Bottom panel) of cortical (left) and hippocampal (right) cultures stimulated with 30 µM NMDA for 60 minutes, were stained with antibodies against p65 (red), MAP2 (neurons, green) or GFAP (astrocytes, green). Cell nuclei were stained with DAPI (blue). The fluorescence intensity in the ROI (i.e., the DAPI-positive region) was quantified. **A)** Representative images of a cortical (left) and hippocampal (right) neuronal cultures stained with p65, MAP2 and DAPI. **B)** Representative images of a cortical (left) and hippocampal (right) astrocyte cultures stained with p65, GFAP and DAPI. **C)** Relative changes of p65 fluorescence intensity in the nuclei of neurons and astrocytes of cortical (CX) and hippocampal (HP) cultures when comparing the stimulated with the control (non-stimulated) condition. Results obtained in n=4 independent experiments. * $p<0.05$ by two-tailed t-test.

Supplementary Figure S3. The expression levels of NF-κB subunit p65 in homogenates and of IkB-α in cytoplasmic fractions remain constant in all conditions. A) and B) Representative Western blots and densitometric quantification of cytoplasmic content of IkB-α in cortical (A) and hippocampal (B) cultures stimulates with NMDA 100 µM in presence or absence of NO inhibitor LNIO (N5-(1-Iminoethyl)-L-ornithine). **C) and D)** Representative Wester blots and densitometric quantification of total content of p65 in cortical (C) and hippocampal (D) cultures stimulates with NMDA 100 µM in presence or absence of NO inhibitor LNIO. For each Western blot, equal quantities of protein were

loaded, and β-III tubulin was used as loading control for cytoplasmic fraction and homogenate.

Supplementary Figure S4. Time course of IL-1β mRNA upregulation in response to NMDA in hippocampal cultures. A) and B) IL-1β mRNA (left) and BAX mRNA (right) measured by quantitative PCR in hippocampal cultures 1, 2 and 6 hours after 100 µM NMDA stimuli. Bar graphs show the mean ± SEM fold change normalized against GAPDH as reference. Data was obtained from 2 to 4 independent hippocampal cultures. Statistical significance was assessed by One-way ANOVA followed by Bonferroni post-test. **p<0.01.

REFERENCES

1. Akhand AA, Pu M, Senga T, Kato M, Suzuki H, Miyata T, Hamaguchi M, Nakashima I (1999) Nitric oxide controls src kinase activity through a sulfhydryl group modification-mediated Tyr-527-independent and Tyr-416-linked mechanism. The Journal of biological chemistry.274(36):25821-6.
2. Ba M, Ding W, Guan L, Lv Y, Kong M (2019) S-nitrosylation of Src by NR2B-nNOS signal causes Src activation and NR2B tyrosine phosphorylation in levodopa-induced dyskinetic rat model. Human & experimental toxicology.38(3):303-10.
3. Balcerczyk A, Soszynski M, Bartosz G (2005) On the specificity of 4-amino-5-methylamino-2',7'-difluorofluorescein as a probe for nitric oxide. Free radical biology & medicine.39(3):327-35.
4. Bhakar AL, Tannis LL, Zeindler C, Russo MP, Jobin C, Park DS, MacPherson S, Barker PA (2002) Constitutive nuclear factor-kappa B activity is required for central neuron survival. The Journal of neuroscience : the official journal of the Society for Neuroscience.22(19):8466-75.
5. Calabrese V, Mancuso C, Calvani M, Rizzarelli E, Butterfield DA, Stella AM (2007) Nitric oxide in the central nervous system: neuroprotection versus neurotoxicity. Nature reviews Neuroscience.8(10):766-75.
6. Caviedes A, Varas-Godoy M, Lafourcade C, Sandoval S, Bravo-Alegria J, Kaehne T, Massmann A, Figueroa JP, Nualart F, Wyneken U (2017) Endothelial Nitric Oxide Synthase Is Present in Dendritic Spines of Neurons in Primary Cultures. Frontiers in cellular neuroscience.11:180.
7. Coultrap SJ, Bayer KU (2014) Nitric oxide induces Ca2+-independent activity of the Ca2+/calmodulin-dependent protein kinase II (CaMKII). The Journal of biological chemistry.289(28):19458-65.
8. Choi YB, Lipton SA (2000) Redox modulation of the NMDA receptor. Cellular and molecular life sciences : CMLS.57(11):1535-41.
9. Chong CM, Ai N, Ke M, Tan Y, Huang Z, Li Y, Lu JH, Ge W, Su H (2018) Roles of Nitric Oxide Synthase Isoforms in Neurogenesis. Molecular neurobiology.55(3):2645-52.
10. Dresselhaus EC, Meffert MK (2019) Cellular Specificity of NF-kappaB Function in the Nervous System. Frontiers in immunology.10:1043.
11. Dudzinski DM, Igarashi J, Greif D, Michel T (2006) The regulation and pharmacology of endothelial nitric oxide synthase. Annual review of pharmacology and toxicology.46:235-76.
12. Figueiredo-Freitas C, Dulce RA, Foster MW, Liang J, Yamashita AM, Lima-Rosa FL, Thompson JW, Moseley MA, Hare JM, Nogueira L, Sorenson MM, Pinto JR (2015) S-Nitrosylation of Sarcomeric Proteins Depresses Myofilament Ca2+)Sensitivity in Intact Cardiomyocytes. Antioxidants & redox signaling.23(13):1017-34.

13. Forrester MT, Foster MW, Stamler JS (2007) Assessment and application of the biotin switch technique for examining protein S-nitrosylation under conditions of pharmacologically induced oxidative stress. The Journal of biological chemistry.282(19):13977-83.
14. Forrester MT, Thompson JW, Foster MW, Nogueira L, Moseley MA, Stamler JS (2009) Proteomic analysis of S-nitrosylation and denitrosylation by resin-assisted capture. Nature biotechnology.27(6):557-9.
15. Forstermann U, Sessa WC (2012) Nitric oxide synthases: regulation and function. European heart journal.33(7):829-37, 37a-37d.
16. Garry PS, Ezra M, Rowland MJ, Westbrook J, Pattinson KT (2015) The role of the nitric oxide pathway in brain injury and its treatment--from bench to bedside. Experimental neurology.263:235-43.
17. Gavalda N, Gutierrez H, Davies AM (2009) Developmental switch in NF-kappaB signalling required for neurite growth. Development.136(20):3405-12.
18. Ghasemi M, Mayasi Y, Hannoun A, Eslami SM, Carandang R (2018) Nitric Oxide and Mitochondrial Function in Neurological Diseases. Neuroscience.376:48-71.
19. Ho GP, Selvakumar B, Mukai J, Hester LD, Wang Y, Gogos JA, Snyder SH (2011) S-nitrosylation and S-palmitoylation reciprocally regulate synaptic targeting of PSD-95. Neuron.71(1):131-41.
20. Huang B, Yang XD, Lamb A, Chen LF (2010) Posttranslational modifications of NF-kappaB: another layer of regulation for NF-kappaB signaling pathway. Cellular signalling.22(9):1282-90.
21. Irie T, Sips PY, Kai S, Kida K, Ikeda K, Hirai S, Moazzami K, Jiramongkolchai P, Bloch DB, Doulias PT, Armoundas AA, Kaneki M, Ischiropoulos H, Kranias E, Bloch KD, Stamler JS, Ichinose F (2015) S-Nitrosylation of Calcium-Handling Proteins in Cardiac Adrenergic Signaling and Hypertrophy. Circulation research.117(9):793-803.
22. Kaltschmidt B, Kaltschmidt C (2015) NF-KappaB in Long-Term Memory and Structural Plasticity in the Adult Mammalian Brain. Frontiers in molecular neuroscience.8:69.
23. Kapadia MR, Eng JW, Jiang Q, Stoyanovsky DA, Kibbe MR (2009) Nitric oxide regulates the 26S proteasome in vascular smooth muscle cells. Nitric Oxide-Biol Ch.20(4):279-88.
24. Kelleher ZT, Matsumoto A, Stamler JS, Marshall HE (2007) NOS2 regulation of NF-kappaB by S-nitrosylation of p65. The Journal of biological chemistry.282(42):30667-72.
25. Kitaoka Y, Kumai T, Kitaoka Y, Lam TT, Munemasa Y, Isenoumi K, Motoki M, Kuribayashi K, Kogo J, Kobayashi S, Ueno S (2004) Nuclear factor-kappa B p65 in NMDA-induced retinal neurotoxicity. Brain research Molecular brain research.131(1-2):8-16.
26. Kitaoka Y, Munemasa Y, Nakazawa T, Ueno S (2007) NMDA-induced interleukin-1beta expression is mediated by nuclear factor-kappa B p65 in the retina. Brain research.1142:247-55.
27. Kneussel M, Wagner W (2013) Myosin motors at neuronal synapses: drivers of membrane transport and actin dynamics. Nature reviews Neuroscience.14(4):233-47.
28. Kors S, Geijtenbeek K, Reits E, Schipper-Krom S (2019) Regulation of Proteasome Activity by (Post-)transcriptional Mechanisms. Front Mol Biosci.6.
29. Li Y, Yu M, Zhao B, Wang Y, Zha Y, Li Z, Yu L, Yan L, Chen Z, Zhang W, Zeng X, He Z (2018) Clonidine preconditioning improved cerebral ischemia-induced learning and memory deficits in rats via ERK1/2-CREB/ NF-kappaB-NR2B pathway. European journal of pharmacology.818:167-73.
30. Marshall HE, Stamler JS (2001) Inhibition of NF-kappa B by S-nitrosylation. Biochemistry.40(6):1688-93.
31. Meberg PJ, Miller MW (2003) Culturing hippocampal and cortical neurons. Methods in cell biology.71:111-27.

32. Meuchel LW, Thompson MA, Cassivi SD, Pabelick CM, Prakash YS (2011) Neurotrophins induce nitric oxide generation in human pulmonary artery endothelial cells. Cardiovascular research.91(4):668-76.
33. Mitre M, Mariga A, Chao MV (2017) Neurotrophin signalling: novel insights into mechanisms and pathophysiology. Clinical science.131(1):13-23.
34. Mnatsakanyan R, Markoutsa S, Walbrunn K, Roos A, Verhelst SHL, Zahedi RP (2019) Proteome-wide detection of S-nitrosylation targets and motifs using bioorthogonal cleavable-linker-based enrichment and switch technique. Nature communications.10(1):2195.
35. Nakamura T, Lipton SA (2016) Nitrosative Stress in the Nervous System: Guidelines for Designing Experimental Strategies to Study Protein S-Nitrosylation. Neurochemical research.41(3):510-4.
36. Nogueira L, Figueiredo-Freitas C, Casimiro-Lopes G, Magdesian MH, Assreuy J, Sorenson MM (2009) Myosin is reversibly inhibited by S-nitrosylation. The Biochemical journal.424(2):221-31.
37. Olloquequi J, Cornejo-Cordova E, Verdaguer E, Soriano FX, Binvignat O, Auladell C, Camins A (2018) Excitotoxicity in the pathogenesis of neurological and psychiatric disorders: Therapeutic implications. Journal of psychopharmacology.32(3):265-75.
38. Paige JS, Xu G, Stancevic B, Jaffrey SR (2008) Nitrosothiol reactivity profiling identifies S-nitrosylated proteins with unexpected stability. Chemistry & biology.15(12):1307-16.
39. Pansiot J, Loron G, Olivier P, Fontaine R, Charriaut-Marlangue C, Mercier JC, Gressens P, Baud O (2010) Neuroprotective effect of inhaled nitric oxide on excitotoxic-induced brain damage in neonatal rat. PloS one.5(6):e10916.
40. Peng Y, Kim JM, Park HS, Yang A, Islam C, Lakatta EG, Lin L (2016) AGE-RAGE signal generates a specific NF-kappaB RelA "barcode" that directs collagen I expression. Scientific reports.6:18822.
41. Perkins ND (2012) Cysteine 38 holds the key to NF-kappaB activation. Molecular cell.45(1):1-3.
42. Qin ZH, Chen RW, Wang Y, Nakai M, Chuang DM, Chase TN (1999) Nuclear factor kappaB nuclear translocation upregulates c-Myc and p53 expression during NMDA receptor-mediated apoptosis in rat striatum. The Journal of neuroscience : the official journal of the Society for Neuroscience.19(10):4023-33.
43. Reynaert NL, Ckless K, Korn SH, Vos N, Guala AS, Wouters EF, van der Vliet A, Janssen-Heininger YM (2004) Nitric oxide represses inhibitory kappaB kinase through S-nitrosylation. Proceedings of the National Academy of Sciences of the United States of America.101(24):8945-50.
44. Sakamoto K, Okuwaki T, Ushikubo H, Mori A, Nakahara T, Ishii K (2017) Activation inhibitors of nuclear factor kappa B protect neurons against the NMDA-induced damage in the rat retina. Journal of pharmacological sciences.
45. Sandoval R, Gonzalez A, Caviedes A, Pancetti F, Smalla KH, Kaehne T, Michea L, Gundelfinger ED, Wyneken U (2011) Homeostatic NMDA receptor down-regulation via brain derived neurotrophic factor and nitric oxide-dependent signalling in cortical but not in hippocampal neurons. Journal of neurochemistry.118(5):760-72.
46. Sen N, Paul BD, Gadalla MM, Mustafa AK, Sen T, Xu R, Kim S, Snyder SH (2012) Hydrogen sulfide-linked sulfhydration of NF-kappaB mediates its antiapoptotic actions. Molecular cell.45(1):13-24.
47. Shevchenko A, Wilm M, Vorm O, Mann M (1996) Mass spectrometric sequencing of proteins silver-stained polyacrylamide gels. Analytical chemistry.68(5):850-8.

48. Smith JG, Aldous SG, Andreassi C, Cuda G, Gaspari M, Riccio A (2018) Proteomic analysis of S-nitrosylated nuclear proteins in rat cortical neurons. Science signaling.11(537).
49. Tabansky I, Liang Y, Frankfurt M, Daniels MA, Harrigan M, Stern S, Milner TA, Leshan R, Rama R, Moll T, Friedman JM, Stern JNH, Pfaff DW (2018) Molecular profiling of reticular gigantocellularis neurons indicates that eNOS modulates environmentally dependent levels of arousal. Proceedings of the National Academy of Sciences of the United States of America.115(29):E6900-E9.
50. Tegeder I (2019) Nitric oxide mediated redox regulation of protein homeostasis. Cellular signalling.53:348-56.
51. Tejeda GS, Esteban-Ortega GM, San Antonio E, Vidaurre OG, Diaz-Guerra M (2019) Prevention of excitotoxicity-induced processing of BDNF receptor TrkB-FL leads to stroke neuroprotection. EMBO molecular medicine.11(7):e9950.
52. Tymianski M (2011) Emerging mechanisms of disrupted cellular signaling in brain ischemia. Nature neuroscience.14(11):1369-73.
53. Wang YR, Qin S, Han R, Wu JC, Liang ZQ, Qin ZH, Wang Y (2013) Cathepsin L plays a role in quinolinic acid-induced NF-Kappab activation and excitotoxicity in rat striatal neurons. PloS one.8(9):e75702.
54. Wu QJ, Tymianski M (2018) Targeting NMDA receptors in stroke: new hope in neuroprotection. Molecular brain.11(1):15.
55. Yu LM, Zhang TY, Yin XH, Yang Q, Lu F, Yan JZ, Li C (2019) Denitrosylation of nNOS induced by cerebral ischemia-reperfusion contributes to nitrosylation of CaMKII and its inhibition of autophosphorylation in hippocampal CA1. European review for medical and pharmacological sciences.23(17):7674-83.
56. Zhang W, Potrovita I, Tarabin V, Herrmann O, Beer V, Weih F, Schneider A, Schwaninger M (2005) Neuronal activation of NF-kappaB contributes to cell death in cerebral ischemia. Journal of cerebral blood flow and metabolism : official journal of the International Society of Cerebral Blood Flow and Metabolism.25(1):30-40.
57. Zhao J, Li X, McGowan S, Niedernhofer LJ, Robbins PD (2015) NF-kappaB activation with aging: characterization and therapeutic inhibition. Methods in molecular biology.1280:543-57.

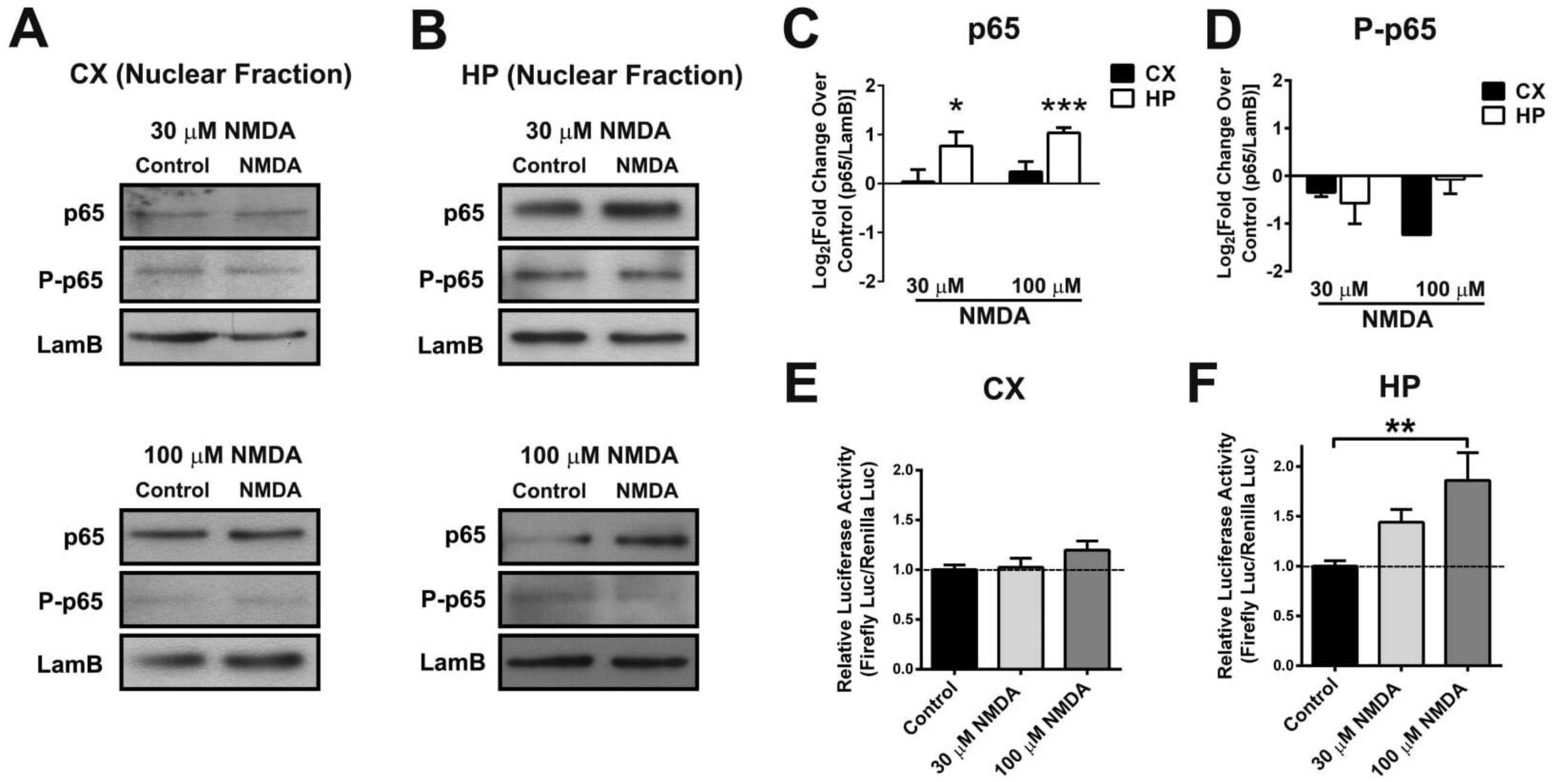
A
CX (Nuclear Fraction)
30 μM NMDA
Control
NMDA
p65
P-p65
LamB
100 μM NMDA
Control
NMDA
p65
P-p65
LamB
B
HP (Nuclear Fraction)
30 μM NMDA
Control
NMDA
p65
P-p65
LamB
100 μM NMDA
Control
NMDA
p65
P-p65
LamB
C
p65
CX
HP
Log2[Fold Change Over Control (p65/LamB)]
2
1
0
-1
-2
*
***
30 μM
100 μM
NMDA
D
P-p65
CX
HP
Log2[Fold Change Over Control (p65/LamB)]
2
1
0
-1
-2
30 μM
100 μM
NMDA
E
CX
Relative Luciferase Activity (Firefly Luc/Renilla Luc)
2.0
1.5
1.0
0.5
0.0
Control
30 μM NMDA
100 μM NMDA
F
HP
**
Relative Luciferase Activity (Firefly Luc/Renilla Luc)
2.0
1.5
1.0
0.5
0.0
Control
30 μM NMDA
100 μM NMDA

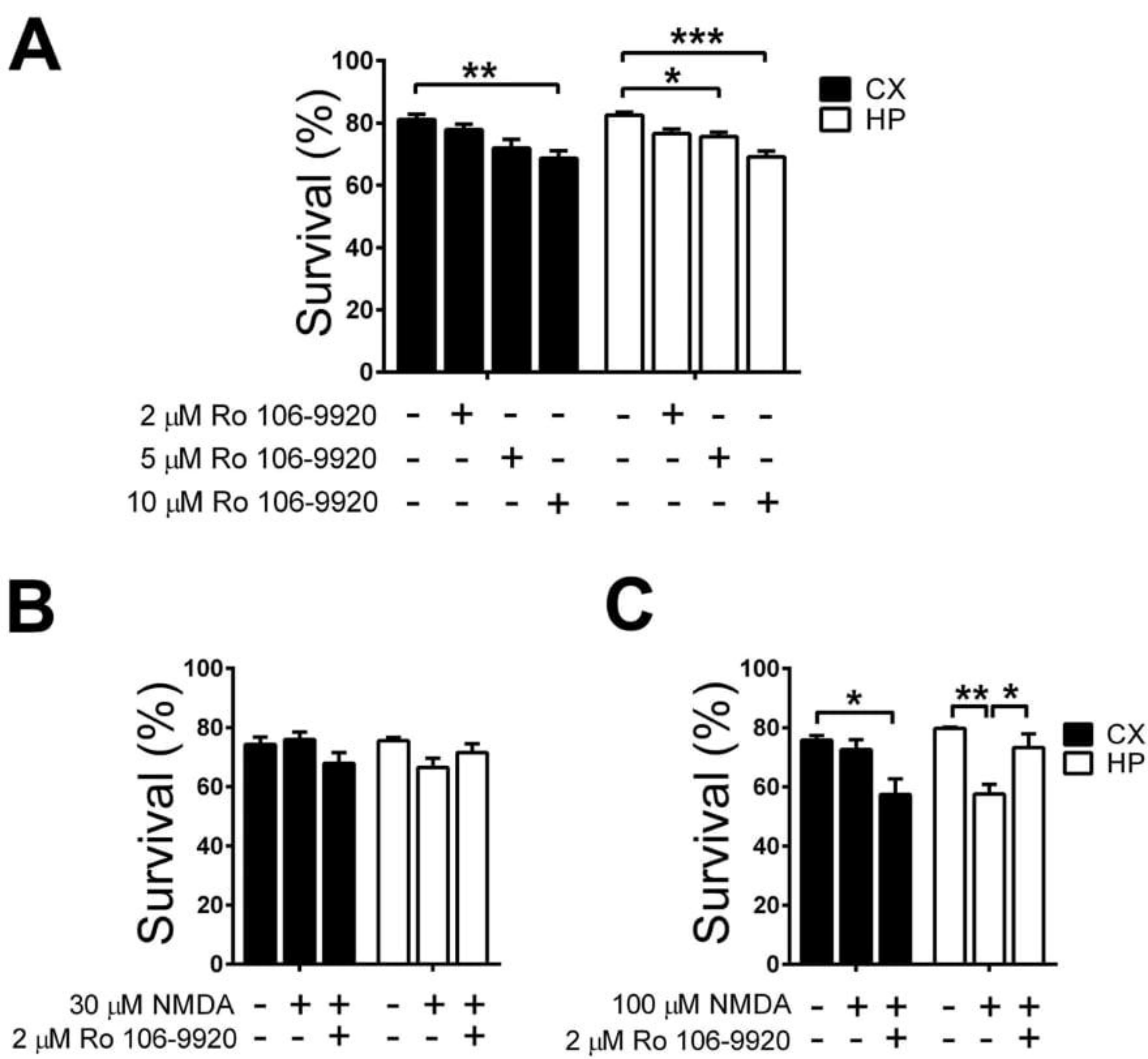
A
Survival (%)
100
80
60
40
20
0
**
***
*
CX
HP
2 μM Ro 106-9920 - + - - - + - -
5 μM Ro 106-9920 - - + - - - + -
10 μM Ro 106-9920 - - - + - - - +
B
Survival (%)
30 μM NMDA - + + - + +
2 μM Ro 106-9920 - - + - - +
C
Survival (%)
*
** *
CX
HP
100 μM NMDA - + + - + +
2 μM Ro 106-9920 - - + - - +

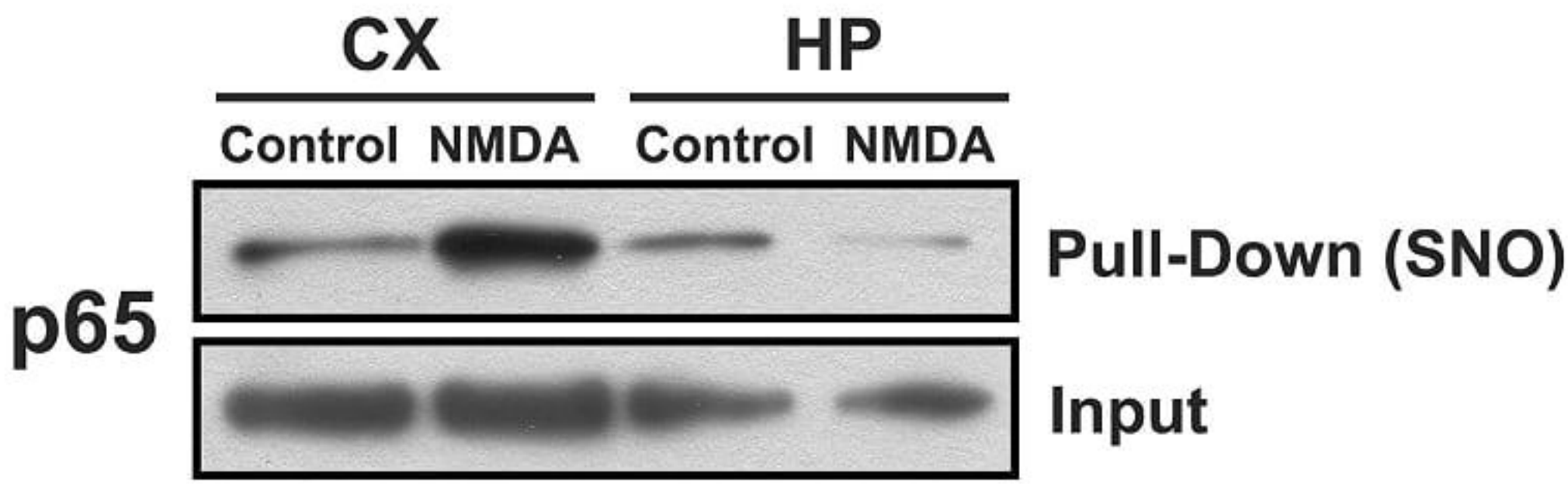
CX
HP
Control
NMDA
Control
NMDA
p65
Pull-Down (SNO)
Input

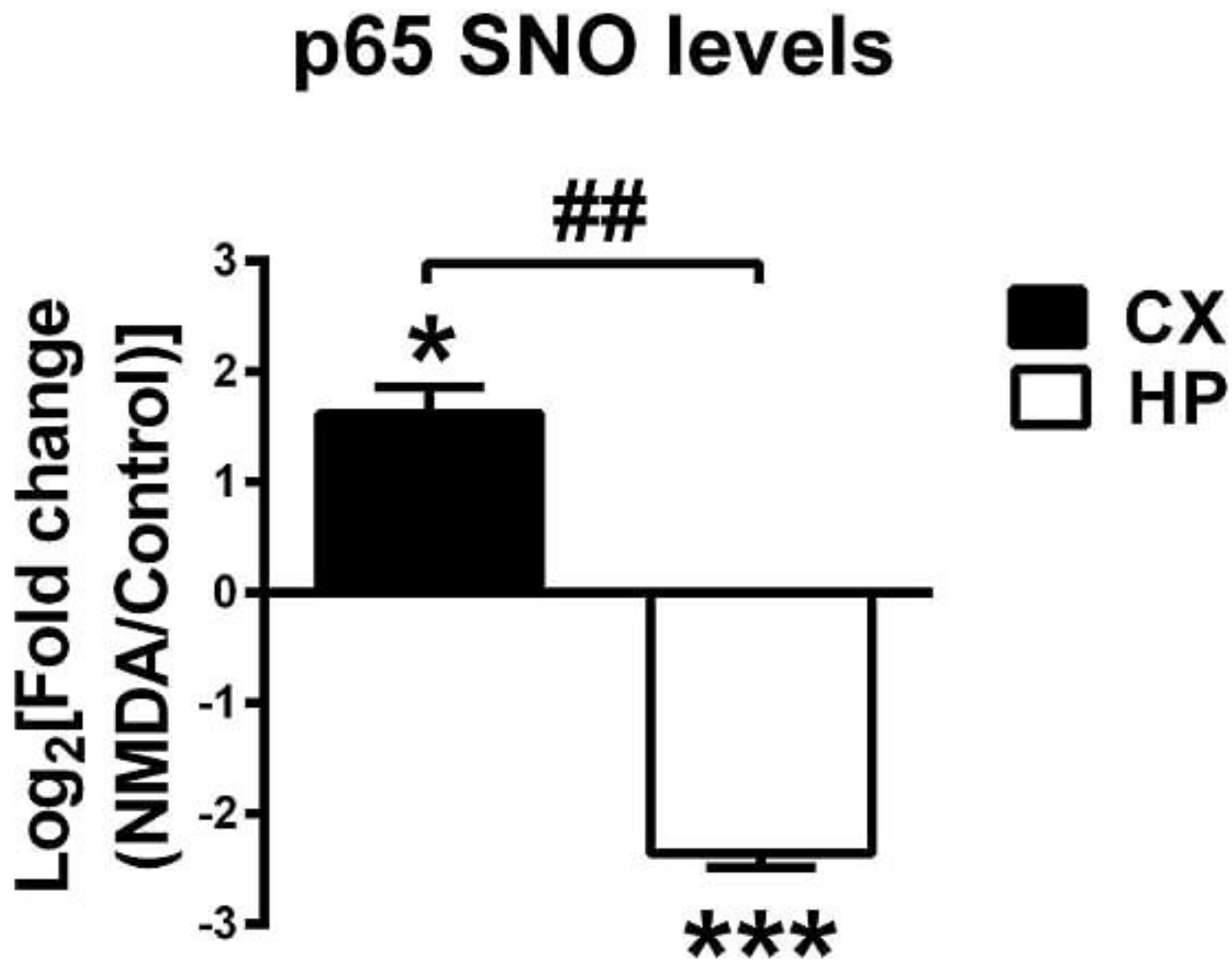
p65 SNO levels
##
*
***
CX
HP
Log2[Fold change
(NMDA/Control)]
3
2
1
0
-1
-2
-3

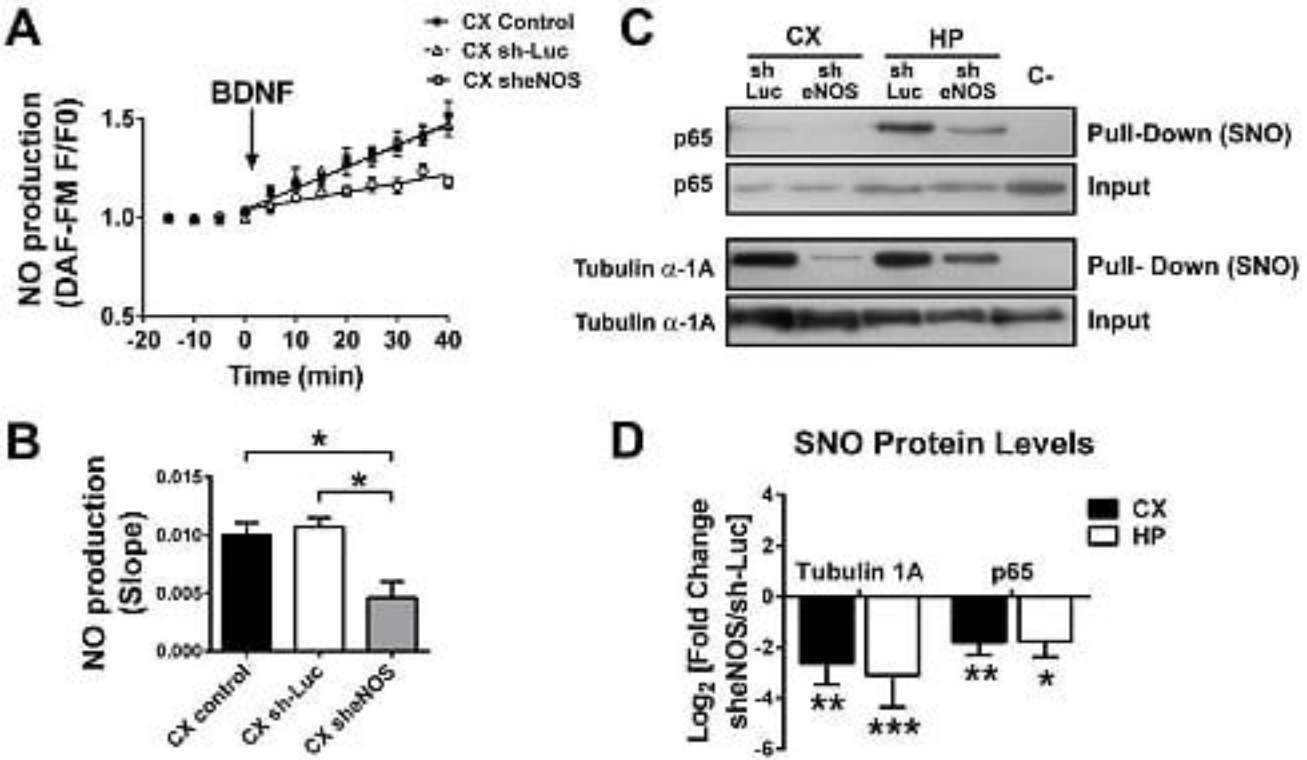
A
CX Control
CX sh-Luc
CX sheNOS
BDNF
NO production (DAF-FM F/F0)
1.5
1.0
0.5
-20 -10 0 10 20 30 40
Time (min)
B
NO production (Slope)
0.015
0.010
0.005
0.000
*
*
CX control
CX sh-Luc
CX sheNOS
C
CX
HP
sh Luc
sh eNOS
sh Luc
sh eNOS
C-
p65
Pull-Down (SNO)
p65
Input
Tubulin α-1A
Pull- Down (SNO)
Tubulin α-1A
Input
D
SNO Protein Levels
CX
HP
Log2 [Fold Change sheNOS/sh-Luc]
4
2
0
-2
-4
-6
Tubulin 1A
p65
**
***
**
*

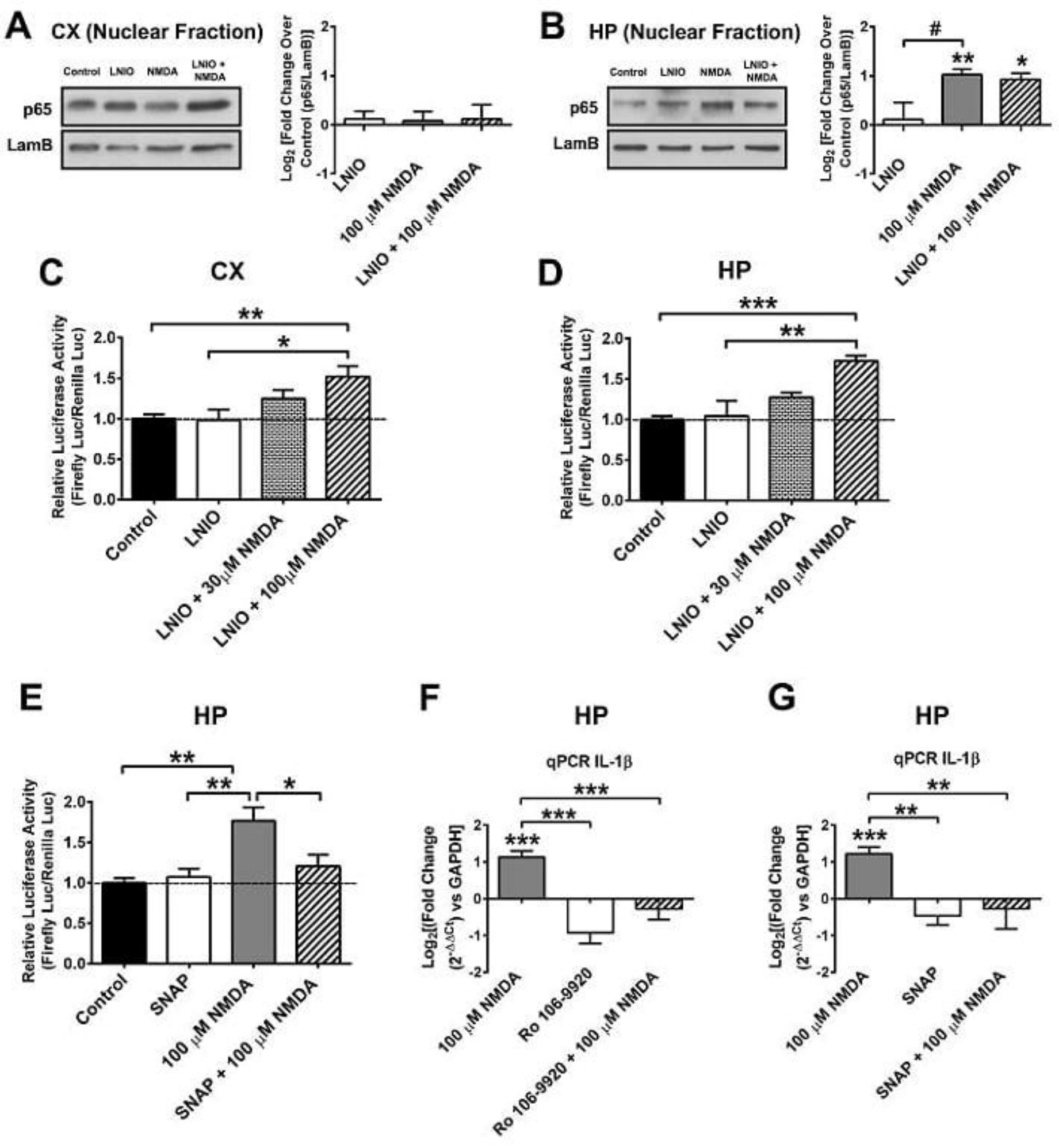
A
CX (Nuclear Fraction)
Control
LNIO
NMDA
LNIO + NMDA
p65
LamB
Log2 [Fold Change Over Control (p65/LamB)]
LNIO
100 μM NMDA
LNIO + 100 μM NMDA
B
HP (Nuclear Fraction)
#
**
*
C
CX
Relative Luciferase Activity (Firefly Luc/Renilla Luc)
LNIO + 30μM NMDA
LNIO + 100μM NMDA
D
HP
***
E
SNAP
SNAP + 100 μM NMDA
F
qPCR IL-1β
Log2[(Fold Change (2-ΔΔCt) vs GAPDH]
Ro 106-9920
Ro 106-9920 + 100 μM NMDA
G

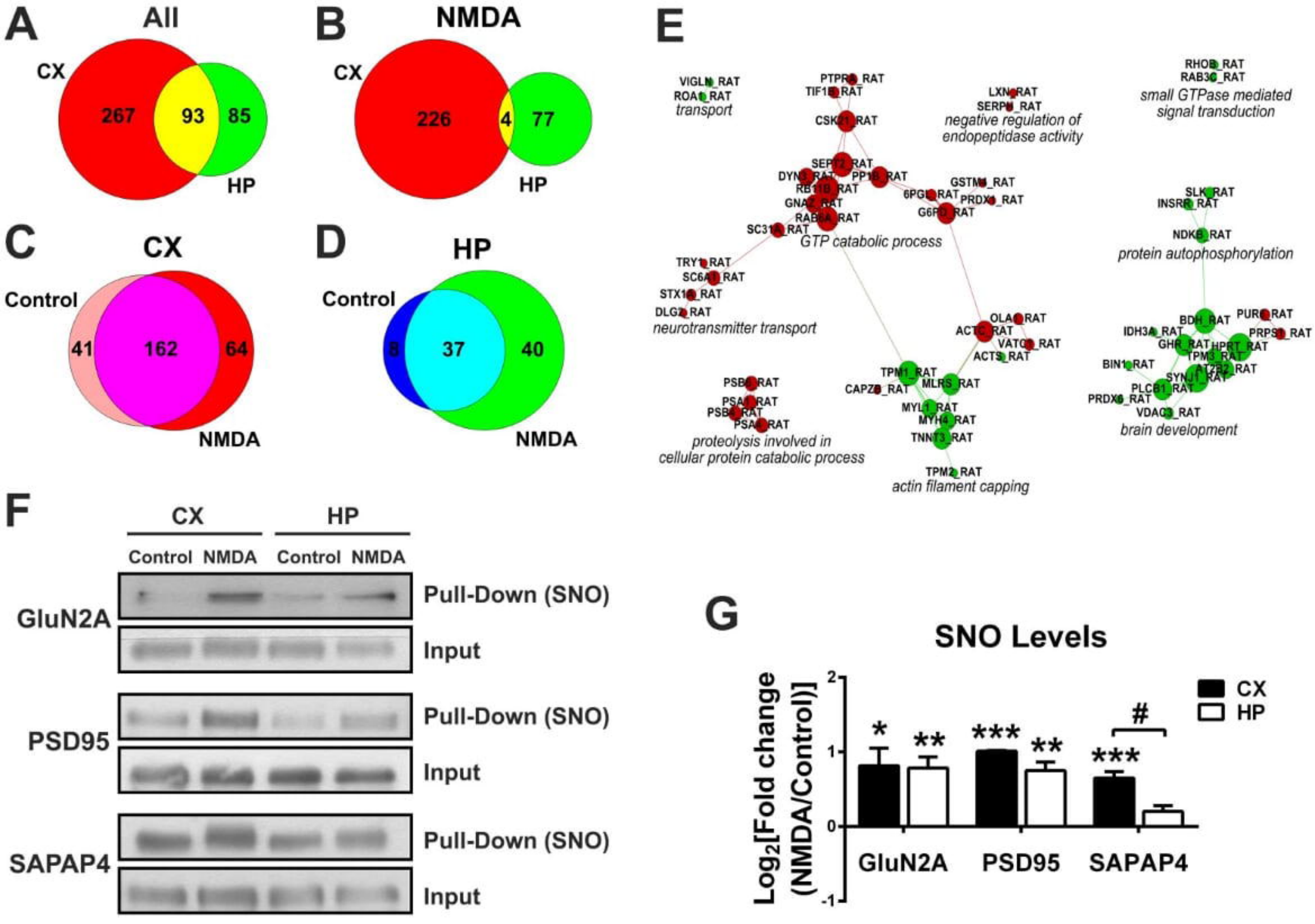
A
All
CX
267
93
85
HP
B
NMDA
CX
226
4
77
HP
C
CX
Control
41
162
64
NMDA
D
HP
Control
8
37
40
NMDA
E
VIGLN_RAT
ROA1_RAT
transport
PTPRA_RAT
TIF1B_RAT
CSK21_RAT
LXN_RAT
SERPN_RAT
negative regulation of endopeptidase activity
RHOB_RAT
RAB3C_RAT
small GTPase mediated signal transduction
SEPT2_RAT
DYN3_RAT
PP1B_RAT
RB11B_RAT
GNAZ_RAT
RAB6A_RAT
SC31A_RAT
GSTM1_RAT
6PGL_RAT
PRDX1_RAT
G6PD_RAT
GTP catabolic process
SLK_RAT
INSRR_RAT
NDKB_RAT
protein autophosphorylation
TRY1_RAT
SC6A1_RAT
STX1B_RAT
DLG2_RAT
neurotransmitter transport
OLA1_RAT
ACTC_RAT
VATG1_RAT
ACTS_RAT
BDH_RAT
PURA_RAT
IDH3A_RAT
PRPS1_RAT
GHR_RAT
HPRT_RAT
TPM3_RAT
BIN1_RAT
ATZR2_RAT
SYNJ1_RAT
PLCB1_RAT
PRDX6_RAT
VDAC3_RAT
brain development
TPM1_RAT
CAPZB_RAT
MLRS_RAT
MYL1_RAT
MYH4_RAT
TNNT3_RAT
TPM2_RAT
actin filament capping
PSB6_RAT
PSA7_RAT
PSB3_RAT
PSA6_RAT
proteolysis involved in cellular protein catabolic process
F
CX
HP
Control
NMDA
Control
NMDA
GluN2A
Pull-Down (SNO)
Input
PSD95
Pull-Down (SNO)
Input
SAPAP4
Pull-Down (SNO)
Input
G
SNO Levels
Log2[Fold change (NMDA/Control)]
2
1
0
-1
*
**
***
**
***
#
CX
HP
GluN2A
PSD95
SAPAP4

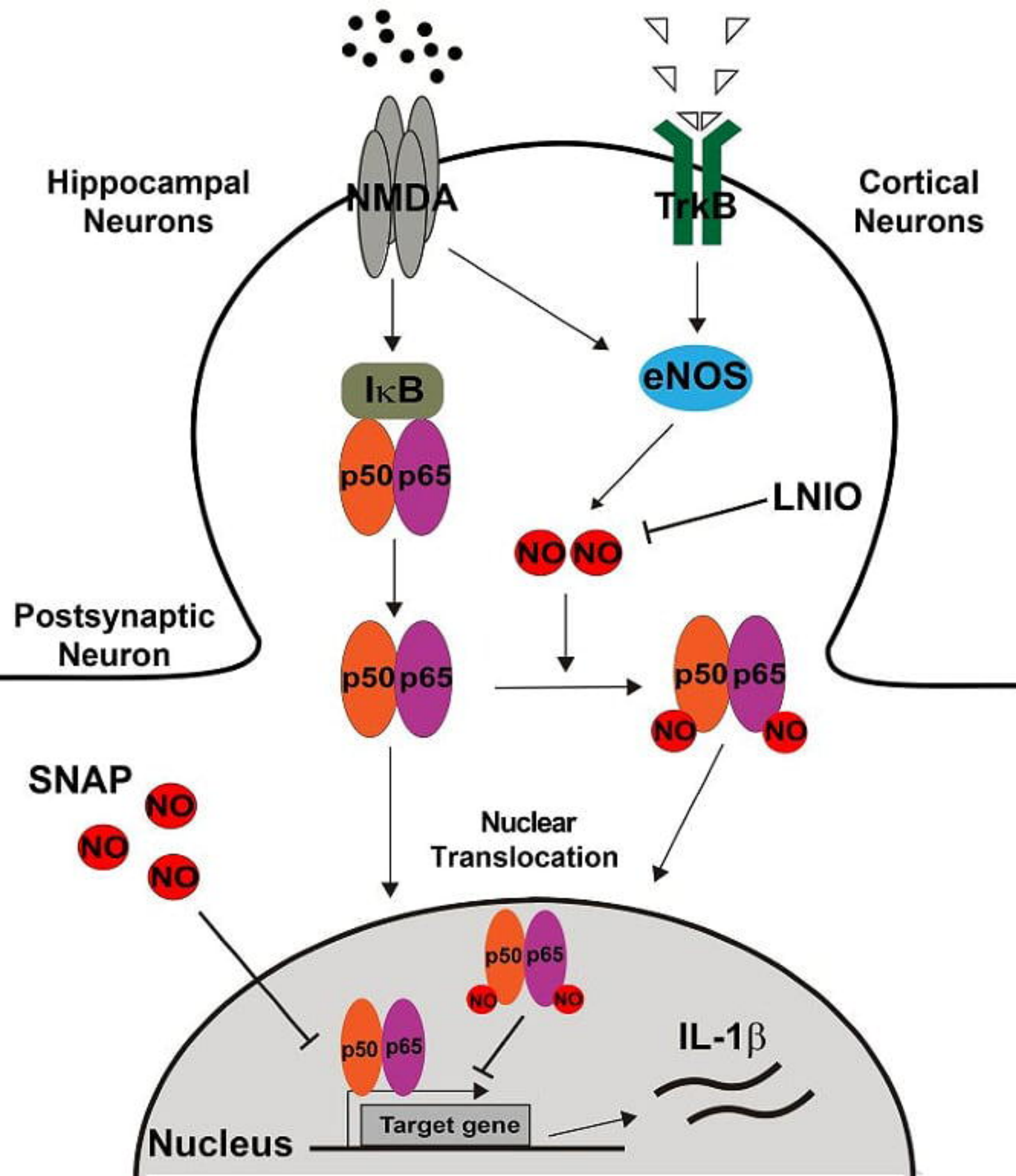
Hippocampal Neurons
NMDA
TrkB
Cortical Neurons
IκB
eNOS
p50 p65
LNIO
NO NO
Postsynaptic Neuron
p50 p65
p50 p65
NO NO
SNAP
NO
NO
NO
Nuclear Translocation
p50 p65
NO NO
p50 p65
IL-1β
Target gene
Nucleus